

# Diffusion of iron in $\text{Cr}_2\text{O}_3$ : polycrystals and thin films

A.C.S. Sabioni<sup>a</sup>, A.M. Huntz<sup>b,\*</sup>, F. Silva<sup>a</sup>, F. Jomard<sup>c</sup>

<sup>a</sup> Laboratório de Difusão em Materiais, Departamento de Física, ICEB-UFOP, Redemat, 35400-000 Ouro Preto, MG, Brazil

<sup>b</sup> Laboratoire d'Etude des Matériaux Hors-Équilibre, LEMHE, CNRS UMR 8647, Université Paris XI, 91405 Orsay, France

<sup>c</sup> Laboratoire de Physique des Solides et Cristallographie, CNRS UPR, Meudon-Bellevue, France

Received 8 June 2004; received in revised form 13 September 2004; accepted 22 September 2004

## Abstract

Chromia protective layers are formed on many industrial alloys to prevent corrosion by oxidation. The role of such layers is to limit the inward diffusion of oxygen and the outward diffusion of cations. A number of chromia-forming alloys contain iron as a major component, such as the stainless steels. To check if chromia is a barrier to the outward diffusion of iron in these alloys, iron diffusion in chromia was studied in both polycrystals and oxide films formed by oxidation of Ni–30Cr alloy in the temperature range 700–1100 °C at an oxygen pressure equal to  $10^{-4}$  atm. An iron film of about 80 nm thick was deposited on the chromia surface, and after the diffusing treatment, iron depth profiles were established by secondary ion mass spectrometry (SIMS). Two diffusion domains appear whatever the nature of the chromia material, polycrystals or films. In the first domain, using a solution of the Fick's second law for diffusion from a thick film, effective or bulk diffusion coefficients were determined. With the second domain, Le Claire's and Hart's models allowed both the bulk diffusion coefficient and the grain-boundary diffusion parameter ( $\alpha D_{\text{gb}}\delta$ ) to be obtained. Iron bulk and grain-boundary diffusion does not vary significantly according to the microstructure of chromia. The activation energy of grain-boundary diffusion is at least equal or even greater than the activation energy of bulk diffusion, probably on account of segregation phenomena. Iron diffusion was compared to cationic self-diffusion in the bulk and along grain boundaries and related to the protective character of chromia.

© 2004 Elsevier B.V. All rights reserved.

**Keywords:** Diffusion; Chromia; Polycrystals; Films; Iron

## 1. Introduction

Chromia films are of great importance as the protection ensured by such films against oxidizing and aggressive atmospheres is efficient for long times at temperatures as high as 1000 °C. Above 1000 °C, vaporisation phenomena occur [1]. Vaporisation is promoted by the presence of water vapor. But, at temperatures lower than 1000 °C, chromia films are amongst the more efficient natural protectors. Thus, chromium is particularly added to stainless steels with the aim of developing a continuous chromia film rather than films of iron oxides whose growth is faster than the growth kinetics of chromia films. For similar reasons, chromium is added to nickel-based alloys, thus coupling good mechanical proper-

ties and oxidation resistance at high temperatures. Besides, chromia films present great advantages in carburisation conditions (cokage) as the formation of a chromia scale, instead of iron or nickel oxides, induces a significant decrease of the amount of carbon deposition [2]. In nearly all these conditions, iron is incorporated in the chromia scales during their growth on iron based alloys and steels, and it is important to know the diffusion rate of iron in such protective scales. This is even more important in the case of chromia films deposited by various coating processes. The lifetime of the coating will clearly depend on the diffusion rate of the various elements through the protective film. Moreover, as iron is a transition element with a size close to that of chromium, iron diffusion in chromia can be representative of the order of magnitude of cation diffusion in chromia and provides evidence of the influence of parameters such as grain size, the presence of impurities, temperature, oxygen pressure and so on.

\* Corresponding author. Tel.: +33 1 69 15 63 18; fax: +33 1 69 15 48 19.  
E-mail address: am.huntz@lemhe.u-psud.fr (A.M. Huntz).

That is why experiments of iron diffusion in chromia were performed from 740 to 1100 °C. In most cases, diffusion was studied in polycrystals in order to obtain bulk and intergranular diffusion coefficients in a compact chromia matrix and some attempts were made with oxide films previously developed on NiCr alloys. The results will be compared to the most recent results obtained for self-diffusion either in massive chromia [3–5] or in chromia layers grown by oxidation, or even hetero-diffusion in layers [6–8].

## 2. Experimental

### 2.1. Material

The synthetic polycrystalline chromia samples used in this work are of the same batch used in a previous study for measuring Cr self-diffusion in  $\text{Cr}_2\text{O}_3$  grain-boundaries [3–5]. These  $\text{Cr}_2\text{O}_3$  polycrystals were prepared by hot pressing at 1450 °C, under 48 MPa, for 40 min, using high-purity powder (99.999%) supplied by Johnson Matthey Corporation. These samples have a density close to the theoretical density of  $\text{Cr}_2\text{O}_3$ , i.e.  $5.21 \text{ g cm}^{-3}$ , and a grain size of ca.  $6 \mu\text{m}$ .

The iron diffusion experiments were also performed on  $\text{Cr}_2\text{O}_3$  layers grown by oxidation of a Ni–30Cr alloy provided by Imphy S.A., and containing some silicon ( $\approx 1.46 \text{ wt.}\%$ ). The NiCr samples were firstly annealed for 3 days in an  $\text{Ar-H}_2\text{-H}_2\text{O}$  atmosphere at 900 °C ( $p_{\text{O}_2} \approx 10^{-19} \text{ atm}$ ), in order to stabilise the grain size of the metallic substrate. Then, these samples were oxidized in laboratory air at 900 °C for 112 h. According to literature data [9], 30% Cr in nickel is sufficient to lead to the growth of  $\text{Cr}_2\text{O}_3$  alone as a continuous film. Indeed,  $N_{\text{Cr} \rightarrow \text{Cr}_2\text{O}_3}^{\text{Min}}$ , the minimum chromium amount in the nickel based alloy necessary to give a continuous chromia film on the surface was calculated as 0.3 in Ref. [9]. Moreover, it was shown that addition of silicon promotes the formation of a  $\text{Cr}_2\text{O}_3$  film [10]. As shown in Fig. 1 concerning the oxi-

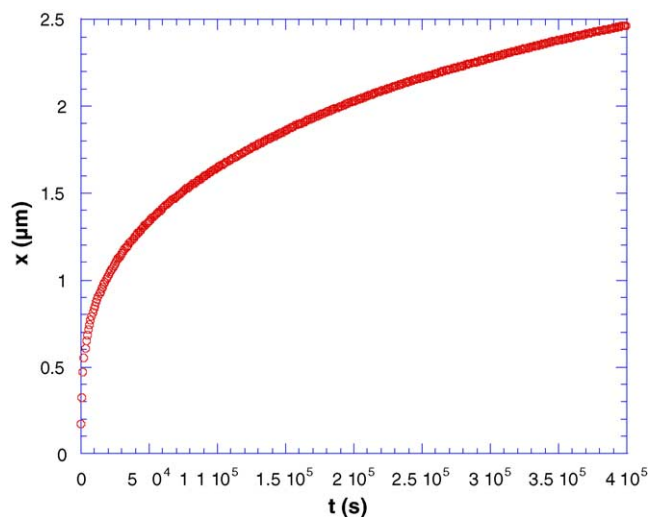


Fig. 1. Oxidation kinetics of Ni–30Cr at 900 °C.

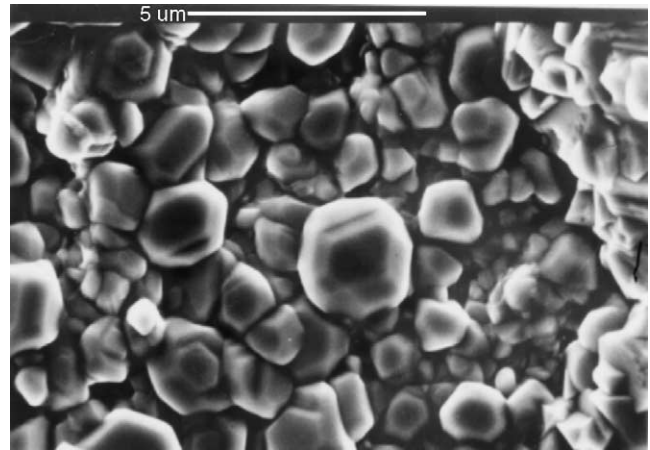


Fig. 2. Microstructure (SEM) of the outer surface of the chromia scale formed at 900 °C on Ni–30Cr alloy.

dation kinetics of such NiCr samples, the oxygen weight gain and consequently the chromia film thickness obey a parabolic law and, at the end of this treatment, the chromia layer is about  $2.5 \mu\text{m}$  thick, with an average grain size of  $\approx 1 \mu\text{m}$ . As shown in Fig. 2, the chromia layer is compact and its roughness is about  $1 \mu\text{m}$ . The defect structure of the chromia film prepared under these conditions is expected to be not far from that of polycrystals, but impurities could be incorporated in the oxide film and modify the defect structure. It is one of the objectives of this work to clarify this point.

### 2.2. Sample preparation

For synthetic polycrystalline chromia, samples  $4 \text{ mm} \times 4 \text{ mm} \times 2 \text{ mm}$  were polished in an automatic grinder/polisher Phoenix 4000/Buehler. Polishing was performed using diamond suspensions of 15, 6, 3, 1, and  $0.25 \mu\text{m}$ . For chromia films, diffusion experiments were made directly on as-oxidised samples. The samples were pre-annealed at the same oxygen pressures and temperatures to be used in the diffusion anneals. Then an electron-beam evaporated iron film was deposited on the polished surface using an AUTO 306 vacuum coater with a turbomolecular pumping system. High purity iron (99.998%), supplied by Alfa Aesar (Johnson Matthey), was used in these experiments. The thickness of the iron film is less than 100 nm, around 70 nm as shown in Fig. 3.

### 2.3. Diffusion experiments

The iron diffusion experiments were performed from 720 to 1100 °C in a tubular furnace. The sample was placed in a Pt crucible inside a silica tube. The partial pressure of oxygen was 10 Pa in most cases. This oxygen pressure was obtained by using a standard mixture of  $\text{Ar}/100 \text{ ppm O}_2$ . An isolated test was performed in an oxygen partial pressure of  $10^5 \text{ Pa}$ , in pure oxygen, at 1000 °C, in order to check any influence of the oxygen pressure on the iron diffusivity in  $\text{Cr}_2\text{O}_3$ .

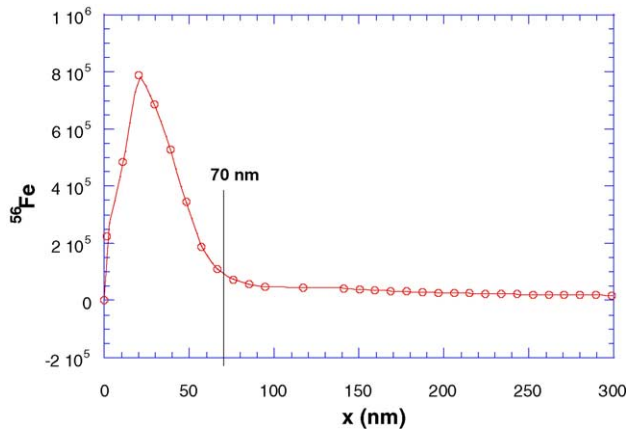


Fig. 3. Iron profile, determined by SIMS, of the iron deposit on Ni–Cr alloy showing that the iron distribution extends to about 70 nm.

#### 2.4. Depth profiling by secondary ion mass spectrometry (SIMS)

The iron depth profiles were established by secondary ion mass spectrometry (SIMS-Cameca 4F-CNRS/Meudon/France), using a 10 keV  $O^{2+}$  primary ion source.

The scanned area was ca.  $250 \mu m \times 250 \mu m$  and the analyzed zone was  $62 \mu m$  in diameter. The iron depth profiles were established with the  $^{56}Fe^-$  signals. The depth of the craters formed on the surface of the samples after SIMS analysis was measured by means of a Talystep profilometer. This allowed the iron intensity to be plotted as a function of the depth in the oxide.

#### 2.5. Determination of bulk and grain-boundary diffusion coefficients

In our experimental conditions, the iron diffusion profiles show two distinct regions (Fig. 4). Near the surface, there is a fast decrease of the concentration, and, far from the surface,

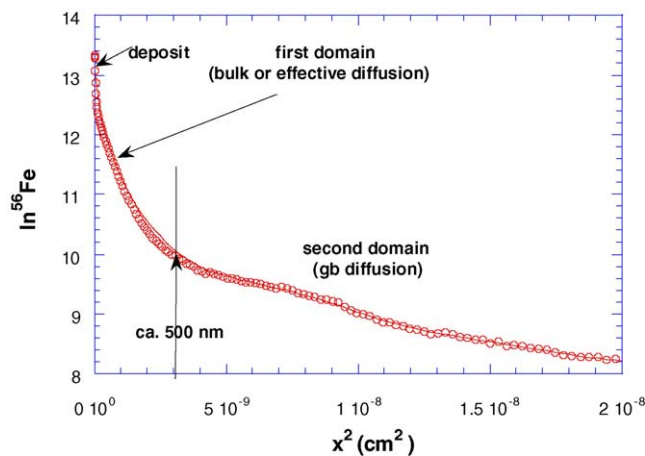


Fig. 4. In Fe as a function of  $x^2$  in the case of a diffusion treatment at  $900^\circ C$  on a chromia film. It shows that the penetration profile consists of two domains.

the concentration slowly decreases. The concentration near the surface should correspond to the contribution of the bulk diffusion, while the concentration far from the surface, i.e. the curve tail, should correspond to grain-boundary diffusion.

However, it sometimes may happen that grain-boundary diffusion contributes to the first part of the concentration profile. One reason for that is related to the grain size. The smaller the grain size, the greater the number of grain-boundaries and, consequently, the greater will be the diffusion in the material along the grain-boundaries and, then, the bulk diffusion from grain boundaries. This is particularly the case for the  $Cr_2O_3$  scales grown by oxidation on Cr alloys, which are comprised of small grains, typically  $1 \mu m$  max.

In order to evaluate the effect of the grain-boundaries on the iron diffusion in  $Cr_2O_3$ , the following procedure was used:

- From the first part of the diffusion profile, a diffusion coefficient was determined using an appropriate solution of the diffusion equation. This diffusion coefficient can correspond either to a bulk diffusion coefficient or to an effective diffusion coefficient, i.e. bulk diffusion with a contribution from grain-boundary diffusion, according to the grain size and to the regime diffusion.

In our experimental conditions, the iron film is thick in comparison with the depth of the first part of the diffusion profile (compare Figs. 3 and 4). So, the diffusion coefficient ( $D$ ) was determined using a solution of the Fick's second law for diffusion from a thick film, given by [11]:

$$C(x, t) = \frac{C_0}{2} \left( \operatorname{erf} \frac{a-x}{2\sqrt{Dt}} + \operatorname{erf} \frac{a+x}{2\sqrt{Dt}} \right), \quad (1)$$

where  $C_0$  is the concentration at the surface,  $a$  is the thickness of the film, and  $D$  is the diffusion coefficient. The  $D$ -values were determined by nonlinear fitting of Eq. (1) to the  $^{56}Fe$  depth profiles using the software Origin (Origin, Data analysis and Technical Graphics in Windows, version 6.0).

- Le Claire's model was used to determine the product  $D_{gb}\delta$  from the tail of the profile, where  $D_{gb}$  is the grain-boundary diffusion coefficient and  $\delta$  is the grain-boundary width, given by [12]:

$$D_{gb}\delta = 0.661 \left[ -\frac{\partial(\ln C)}{\partial x^{6/5}} \right]^{-5/3} \left( \frac{4D_b}{t} \right)^{1/2}. \quad (2)$$

In fact, as our work is focused on hetero-diffusion in polycrystalline materials, the so-determined diffusion parameter corresponds to  $\alpha D_{gb}\delta$ , where  $\alpha$  is a dimensionless parameter known as segregation factor [11].

In the polycrystalline chromia samples, with a grain size of about  $6 \mu m$ , intergranular diffusion in the first diffusion domain is negligible. Thus, Eq. (1) leads to  $D_b$  and Eq. (2) to  $\alpha D_{gb}\delta$ .

But, in case of chromia films, as the grain size is smaller ( $\leq 1 \mu m$ ) the first part of the penetration curve leads to an effective diffusion coefficient, so that a third equation is

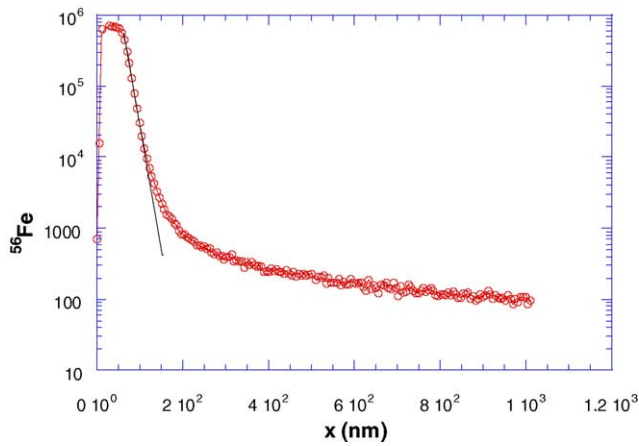


Fig. 5. Iron penetration profile established by SIMS after diffusion treatment at 900 °C. Case of a polycrystalline chromia sample.

necessary to solve Eq. (2) and to obtain bulk and grain-boundary diffusion coefficients.

- (c) Hart's equation [13] was used to relate the effective diffusion coefficient with the bulk diffusion coefficient ( $D_b$ ) and with the grain-boundary diffusion coefficient through the following relationship:

$$D_{\text{eff}} = f\alpha D_{\text{gb}} + (1 - f)D, \quad (3)$$

where  $f$  is the fraction of atomic sites located on the grain-boundaries. For a polycrystal with a grain-size  $\phi$ ,  $f$  may be calculated from the relation  $f = 3\delta/\phi$  [11]. The grain-boundary width ( $\delta$ ) is usually assumed to be 1 nm [14]. Thus,  $f$  is taken as  $5 \times 10^{-4}$  and  $3 \times 10^{-3}$  for the polycrystals and the chromia films, respectively.

$D_b$  and  $\alpha D_{\text{gb}}$  were determined by solving Eqs. (2) and (3) introducing in the software Origin the following data:  $D_{\text{eff}}$ ,  $t$ ,  $f$  and  $[\partial(\ln C)/\partial x^{6/5}]$  (see Fig. 6).

### 3. Results

Fig. 5 shows a diffusion profile of  $^{56}\text{Fe}$  obtained in chromia polycrystals at 900 °C. The profile clearly shows two different diffusion mechanisms as also shown in Fig. 4 in case of iron diffusion in a chromia film. The first part of the profile

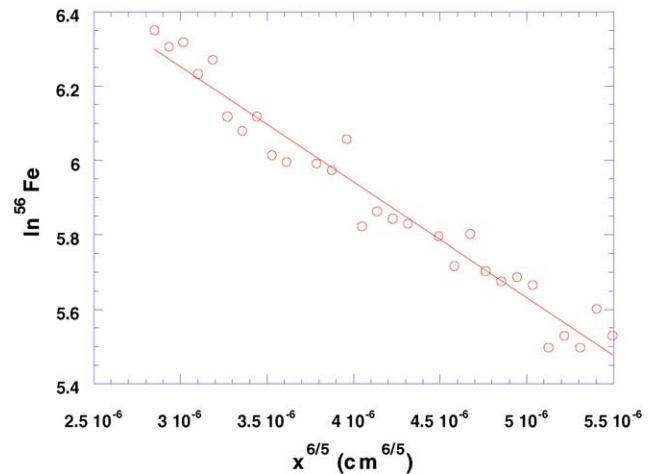


Fig. 6.  $\ln \text{Fe}$  as a function of  $x^{6/5}$  in the case of a diffusion treatment at 900 °C on a chromia polycrystal, showing that the curve tail obeys Eq. (2).

Table 1

Iron diffusion in polycrystalline  $\text{Cr}_2\text{O}_3$ ,  $f = 5 \times 10^{-4}$

$T$ (°C)	$p\text{O}_2$ (atm)	$t$ (s)	$D_b$ ( $\text{cm}^2 \text{s}^{-1}$ )	$\alpha D_{\text{gb}}$ ( $\text{cm}^2 \text{s}^{-1}$ )
740 <sup>a</sup>	$10^{-4}$	$1.7 \times 10^5$	$3.5 \times 10^{-18}$	$5.9 \times 10^{-12}$
800	$10^{-4}$	$8.28 \times 10^4$	$1.1 \times 10^{-17}$	$2.0 \times 10^{-13}$
800	$10^{-4}$	$8.28 \times 10^4$	$1.1 \times 10^{-17}$	$1.6 \times 10^{-11}$
900	$10^{-4}$	$7.20 \times 10^4$	$1.3 \times 10^{-17}$	$1.7 \times 10^{-12}$
1000	$10^{-4}$	$2.19 \times 10^4$	$1.0 \times 10^{-16}$	$4.0 \times 10^{-11}$
1000	1	$2.19 \times 10^4$	$1.2 \times 10^{-16}$	$3.9 \times 10^{-11}$
1100	$10^{-4}$	$1.80 \times 10^4$	$7.3 \times 10^{-16}$	$9.2 \times 10^{-10}$
1100	$10^{-4}$	$1.80 \times 10^4$	$5.9 \times 10^{-16}$	$5.7 \times 10^{-10}$
1100 <sup>a</sup>	$10^{-4}$	$1.80 \times 10^4$	$6.6 \times 10^{-16}$	$7.5 \times 10^{-10}$

<sup>a</sup> Average values.

corresponds to bulk or effective diffusion and the second part of the profile, i.e., the curve tail, is characteristic of the diffusion along grain-boundaries. The gradient  $d \ln C / d \ln x^{6/5}$  of Le Claire's equation was calculated from the tail of the diffusion profile as shown in Fig. 6. Similar profiles were obtained in all cases, whatever the temperature, the oxygen pressure or the nature of the oxide (polycrystal or film).

From all these profiles, according to the procedure explained in Section 2.5, two or three diffusion coefficients were determined: bulk, effective, and grain-boundary diffusion coefficients (in fact  $\alpha D_{\text{gb}}$ ). The values are summarized in Tables 1 and 2 with the characteristics of the test. Arrhe-

Table 2

Iron diffusion in  $\text{Cr}_2\text{O}_3$  films formed on  $\text{Ni}_{70}\text{Cr}_{30}$  alloy,  $f = 3 \times 10^{-3}$

$T$ (°C)	$p\text{O}_2$ (atm)	$t$ (s)	$D_{\text{eff}}$ ( $\text{cm}^2 \text{s}^{-1}$ )	$D_b$ ( $\text{cm}^2 \text{s}^{-1}$ )	$\alpha D_{\text{gb}}$ ( $\text{cm}^2 \text{s}^{-1}$ )
720	$10^{-4}$	$1.449 \times 10^5$	$9.4 \times 10^{-17}$	$1.2 \times 10^{-19}$	$3.1 \times 10^{-14}$
800	$10^{-4}$	$5.760 \times 10^4$	$7.0 \times 10^{-16}$	$1.1 \times 10^{-19}$	$2.3 \times 10^{-13}$
800	$10^{-4}$	$5.760 \times 10^4$	$8.6 \times 10^{-16}$	$2.8 \times 10^{-18}$	$2.9 \times 10^{-13}$
800	$10^{-4}$	$5.760 \times 10^4$	$7.4 \times 10^{-16}$	$2.1 \times 10^{-18}$	$2.4 \times 10^{-13}$
800 <sup>a</sup>	$10^{-4}$	$5.760 \times 10^4$	$7.7 \times 10^{-16}$	$1.7 \times 10^{-18}$	$2.5 \times 10^{-13}$
900	$10^{-4}$	$4.020 \times 10^4$	$8.6 \times 10^{-15}$	$4.1 \times 10^{-18}$	$2.9 \times 10^{-12}$
900	$10^{-4}$	$4.020 \times 10^4$	$1.3 \times 10^{-14}$	$2.7 \times 10^{-17}$	$4.3 \times 10^{-12}$
900	$10^{-4}$	$4.020 \times 10^4$	$5.2 \times 10^{-15}$	$5.7 \times 10^{-20}$	$1.7 \times 10^{-12}$
900 <sup>a</sup>	$10^{-4}$	$4.020 \times 10^4$	$8.9 \times 10^{-15}$	$1.0 \times 10^{-17}$	$3.0 \times 10^{-12}$

<sup>a</sup> Average values.



Table 3

Arrhenius equations for bulk and grain-boundary diffusion

Chromia polycrystal	Chromia film
$D_b \text{ (cm}^2\text{/s)} = 4.3 \times 10^{-9} \exp[-(181 \pm 56) \text{ kJ/RT}]$	$D_{\text{eff}} \text{ (cm}^2\text{/s)} = 7.0 \times 10^{-4} \exp[-(245 \pm 6) \text{ kJ/RT}]$
$\alpha D_{\text{gb}} \text{ (cm}^2\text{/s)} = 1.2 \times 10^4 \exp[-(347 \pm 20) \text{ kJ/RT}]$	$D_b \text{ (cm}^2\text{/s)} = 4.4 \times 10^{-7} \exp[(237 \pm 40) \text{ kJ/RT}]$
	$\alpha D_{\text{gb}} \text{ (cm}^2\text{/s)} = 2.7 \times 10^{-1} \exp[-(249 \pm 8) \text{ kJ/RT}]$

nius equations were established for these different diffusion coefficients and are given in Table 3. Fig. 7 correspond to the Arrhenius plot of the bulk diffusion coefficients. It can be seen that bulk diffusion in chromia is not so different according to the nature of the material (film or massive specimen), but a slight difference is obtained for the activation energy which is equal to 181 and 237 kJ mol<sup>-1</sup> for polycrystals and films, respectively. Nevertheless, the difference occurs mainly at the lowest temperatures, i.e. at 800–740 °C, as shown in Fig. 7b, where the two points relative to diffusion in polycrystals at these temperatures have been suppressed.

Fig. 8 corresponds to the Arrhenius plot of the grain-boundary diffusion coefficients. Again the diffusion values are very close whatever the nature of the chromia, polycrystals or films, but the activation energy differs as it is found

347 kJ mol<sup>-1</sup> in polycrystals and 250 kJ mol<sup>-1</sup> in chromia films.

## 4. Discussion

### 4.1. Difference between iron diffusion in polycrystals and in chromia films formed on NiCr alloys by oxidation

It appears in Figs. 7–8 that iron diffusion in chromia does not really differ according to the nature of chromia, i.e. in chromia as a film or as a massive polycrystalline material, both for bulk and grain-boundary diffusion. Concerning bulk diffusion, this is rather satisfying as bulk diffusion coefficients should not depend on the microstructure. It is not sure that the slight difference which is observed at lower temperatures (740–800 °C, Fig. 7a) is significant. Indeed, it can be seen in Fig. 7b, that the diffusion coefficients obtained for polycrystals in the temperature range 900–1100 °C are aligned with the points obtained in chromia films in the temperature range 720–900 °C. Tsai et al. [8], in their works concerning chromium and oxygen diffusion in chromia films which were slowly cooled after their growth, found bulk diffusion coefficients similar to those obtained in massive polycrystals. But these authors considered a modified *f*-value in the case of films, taking into account the particular roughness of the oxide films. In our case, this is not necessary. If the difference noted at low temperature in Fig. 7a is considered as significant, then it can be attributed to the presence of silicon

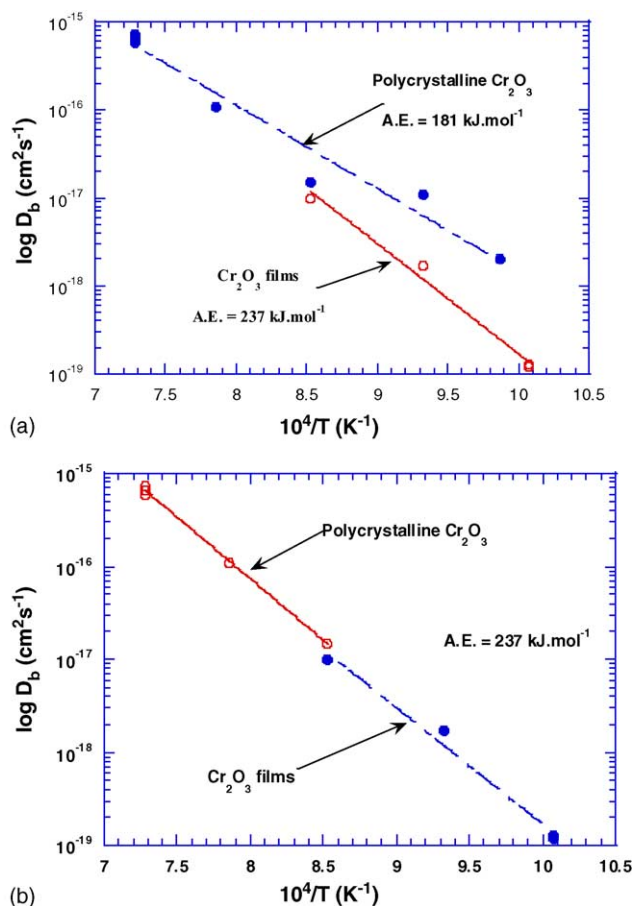


Fig. 7. (a) and (b) Arrhenius plot for bulk diffusion of iron in chromia polycrystals and films. Limited points for diffusion in polycrystalline chromia in (b).

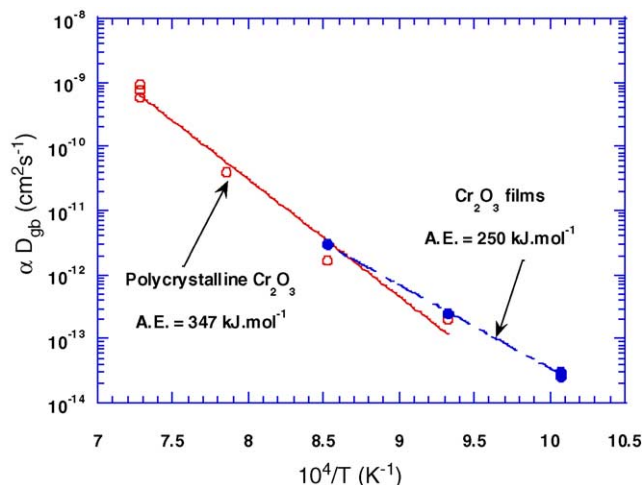


Fig. 8. Arrhenius plot for grain-boundary diffusion of iron in chromia polycrystals and films.

in chromia films which is expected to slow down the diffusion rate. Concerning grain-boundary diffusion, it is important to remark that the penetration curve analyses lead to  $\alpha D_{gb}\delta$ , i.e. to the product of the grain-boundary diffusion coefficient by the boundary width ( $\delta$ ) and by the segregation factor  $\alpha$ . Usually  $\delta$  is taken as equal to  $10^{-7}$  cm, and the segregation factor is unknown and should vary according to temperature and especially according to the impurities that are incorporated in the oxide. Particularly, in the case of films, it should depend on the substrate nature and purity. Consequently, it is rather surprising to obtain similar  $\alpha D_{gb}\delta$ -values for films and polycrystals. Note, however, that it is possible that the agreement occurs only for the studied temperature range. At higher temperatures, grain-boundary diffusion is probably faster in polycrystals and inversely at smaller temperatures.

It also clearly appears that the diffusion activation energy values are obtained with great uncertainty. Indeed, Fig. 7 indicates that, according to the temperature range explored for bulk diffusion in polycrystals, a significant difference is obtained for the activation energy ( $50 \text{ kJ mol}^{-1}$ ). Thus, it is not reasonable to discuss differences in the activation energy for bulk diffusion in polycrystals or in films. It looks like if the bulk diffusion mechanism is similar for both materials. In case of grain-boundary diffusion, the activation energy is greater for massive polycrystals than for thin films,  $374 \text{ kJ mol}^{-1}$  in case of massive polycrystals, instead of  $250 \text{ kJ mol}^{-1}$  for chromia films. In both cases, the activation energy for grain-boundary diffusion is not smaller than the activation energy for bulk diffusion, as expected from theory if the grain boundaries are pure, i.e. without segregation phenomena [11]. Inversely, in the case of polycrystals, the activation energy of grain-boundary diffusion is greater than the activation energy of bulk diffusion (irrespective of whatever the value considered in Fig. 7). Such results were already found in other cases of diffusion in oxides [3–5, 17–18] and are generally attributed to the presence of impurities in grain boundaries.

#### 4.2. Comparison with cation self-diffusion

Fig. 9 and Table 4 allow the comparison of results obtained for chromium diffusion by Tsai et al. [8,15,16] and for iron diffusion in this study. It appears that iron bulk diffusion is slower than chromium diffusion only in the case of chromia films and the difference is small. In the case of polycrystals, there is no significant difference between cation

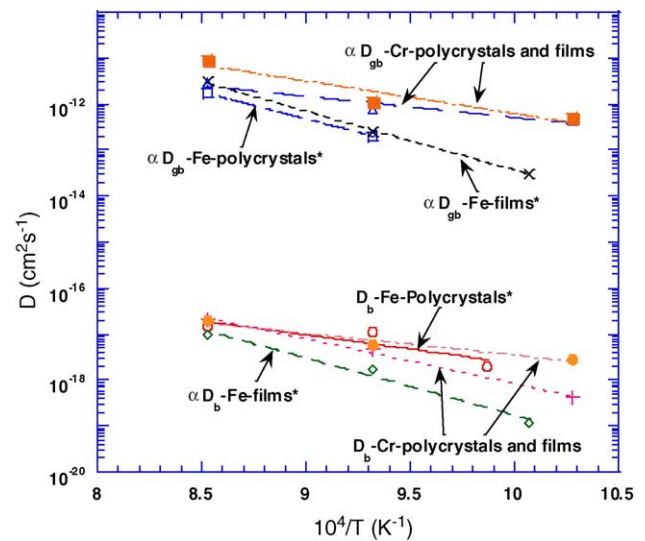


Fig. 9. Comparison, in an Arrhenius plot, of the bulk and grain-boundary diffusion of iron (this work) and chromium [8] in chromia polycrystals and films.

self-diffusion and iron diffusion. Concerning grain-boundary diffusion, a slight tendency for a smaller diffusion of iron, when compared to cation self-diffusion, is observed. These small differences are related to the fact that the ionic radius of the cations  $\text{Cr}^{3+}$ , 0.062 nm, are very close to the ionic radius of  $\text{Fe}^{3+}$ , 0.065 nm [19]. Considering that iron diffuses as  $\text{Fe}^{2+}$  interstitial, as suggested sometimes in the case of iron diffusion in  $\text{Fe}_2\text{O}_3$  [20], should justify that iron diffuses slower than chromium, as its ionic radius is then greater (0.076 nm). Nevertheless, it seems less probable in the case of  $\text{Cr}_2\text{O}_3$  as this oxide is not deficient in oxygen as is  $\text{Fe}_2\text{O}_3$ . The possible differences between the activation energy of cation self-diffusion and iron heterodiffusion will not be discussed on account of the limited temperature range studied for the various materials and the uncertainty on activation energy values already mentioned. Note only, on the basis of results gathered in Fig. 9 for grain-boundary diffusion, that the lower the temperature, the smaller the diffusion of iron when compared to chromium diffusion, suggesting interactions between iron and impurities incorporated in the grain boundaries of chromia.

These results are important to understand the barrier effect of chromia scales. It is well known that chromia films act as an efficient barrier for materials used at high temperatures. For instance, in coal gasification conditions [21], carbon deposi-

Table 4  
Chromium diffusion in chromia polycrystals and in chromia films [7,8,15,16]

$T$ (°C)	$p\text{O}_2$ (atm)	$\text{Cr}_2\text{O}_3$ polycrystals		$\text{Cr}_2\text{O}_3$ films	
		$D_b$	$D_{gb}$	$D_b$	$D_{gb}$
700 [6]	0.1	$4.2 \times 10^{-19}$	$4.4 \times 10^{-13}$	$2.9 \times 10^{-18}$	$5.1 \times 10^{-13}$
800 [6]	0.1	$4.6 \times 10^{-18}$	$7.7 \times 10^{-13}$	$5.9 \times 10^{-18}$	$1.1 \times 10^{-12}$
900 [6]	0.1	$2.1 \times 10^{-17}$	$2.9 \times 10^{-12}$	$2.0 \times 10^{-17}$	$9.3 \times 10^{-12}$
900 [7]	$10^{-15}$			$7 \times 10^{-15}$ , $8 \times 10^{-16}$	$2 \times 10^{-10}$ , $5 \times 10^{-11}$

Table 5  
Various diffusion results at 900 °C

$D$ (cm <sup>2</sup> s <sup>-1</sup> )	$D_{\text{eff}}$	$D_b$	$D_{\text{gb}}$	Oxidation constant $k_c$ (cm <sup>2</sup> s <sup>-1</sup> )
Cr <sub>2</sub> O <sub>3</sub> /Cr, $D^{\text{O}}$ [6]		$1.7 \times 10^{-15}$	$1 \times 10^{-12}$	
Cr <sub>2</sub> O <sub>3</sub> /FeCrNi, $D^{\text{Fe}}$ [7]		$4 \times 10^{-15}$ , $7 \times 10^{-16}$	$1 \times 10^{-10}$	
$D^{\text{Cr}}$		$7 \times 10^{-15}$ , $8 \times 10^{-16}$	$2 \times 10^{-10}$ , $5 \times 10^{-11}$	
$D^{\text{Ni}}$		$5 \times 10^{-15}$ , $4 \times 10^{-16}$	$5 \times 10^{-12}$ , $1 \times 10^{-12}$	
Cr <sub>2</sub> O <sub>3</sub> /FeCr, $D^{\text{Fe}}$ [7]		$2 \times 10^{-14}$ , $3 \times 10^{-15}$	$1 \times 10^{-9}$	
$D^{\text{Cr}}$		$1 \times 10^{-14}$	$1 \times 10^{-9}$	
$D^{\text{Ni}}$		$4 \times 10^{-16}$	$2 \times 10^{-10}$	
Cr <sub>2</sub> O <sub>3</sub> , $D^{\text{Cr}}$ [3–5]		$2 \times 10^{-21}$ = extrapolation	Unreasonable extrapolation	
Cr <sub>2</sub> O <sub>3</sub> , $D^{\text{O}}$		$1 \times 10^{-19}$ = extrapolation	Unreasonable extrapolation	
Cr <sub>2</sub> O <sub>3</sub> , $D^{\text{Cr}}$ [8]		$2.1 \times 10^{-17}$	$2.9 \times 10^{-12}$	
Cr <sub>2</sub> O <sub>3</sub> , $D^{\text{O}}$	$1 \times 10^{-16}$	$8 \times 10^{-18}$	$3 \times 10^{-13}$	
Cr <sub>2</sub> O <sub>3</sub> /NiCr, $D^{\text{Cr}}$		$2.0 \times 10^{-17}$	$9.3 \times 10^{-12}$	
Cr <sub>2</sub> O <sub>3</sub> /NiCr, $D^{\text{O}}$	$1.5 \times 10^{-15}$	$3 \times 10^{-19}$	$4 \times 10^{-13}$	
$k_c$ (cm <sup>2</sup> s <sup>-1</sup> )				$4 \times 10^{-14}$

tion on iron-based alloys is known as particularly enhanced if nickel and/or iron are present on the top of the alloy (or on the top of the oxide film, if the alloy is oxidised). Chromia is known as a good protective scale preventing carbon deposition on iron-based alloys because, in such a case, nickel and iron are not present on the top of the oxide films. The reason could be either kinetic, if chromia acts as a barrier for iron diffusion, or thermodynamic, due to the fact that chromia induces a decrease of the oxygen potential at the iron-oxide film interface so that iron is not oxidised and consequently not incorporated in the film. The results obtained in this study indicate that the thermodynamical effect is the main parameter. Indeed, iron diffuses roughly at the same rate as chromium in chromia, and it can be said that chromia does not act as a specific barrier for iron, compared to chromium diffusion in the oxide film. But iron is not incorporated in the oxide film as the oxygen pressure is too small for the formation of iron oxide and then it cannot diffuse towards the outer surface, consequently carbon deposition is strongly decreased.

Comparison with other literature data (Table 5) were already done by Tsai et al. [8,15,16] who indicated, for instance, that “bulk” diffusion coefficients of chromium or iron in chromia films, determined by Lobnig et al. [7], were related to effective diffusion rather than bulk diffusion. This is again clearly confirmed by the comparison of our results and those of Lobnig in Fig. 10. The values given by these authors are superimposed with our effective diffusion coefficients determined in chromia films.

Concerning anion diffusion, Tsai et al. [8] performed simultaneous experiments of cation and anion diffusion and showed that oxygen diffuses slightly slower in chromia than chromium. The most important feature in relation to the oxidation processes concerns the fact that the oxide film growth, in the temperature range studied here, is mainly governed by grain-boundary diffusion: indeed, the  $k_c$  value is directly related to the diffusion coefficient which predominates [22].

In previous works [3–5], it was suggested that the major cationic point defects in Cr<sub>2</sub>O<sub>3</sub> should be chromium vacancies. In such a case, the bulk cationic diffusion coefficient should vary with the oxygen pressure as  $(p\text{O}_2)^{3/16}$ . This would lead to a diffusion coefficient in 1 atm oxygen equal to 5.6 times the diffusion coefficient in  $10^{-4}$  atm oxygen. Values found for polycrystals at 1000 °C in 1 and  $10^{-4}$  atm oxygen (see Table 1) are not significantly different and indicate that there is no effect of the oxygen pressure on the iron diffusion in chromia.

## 5. Conclusion

Iron diffusion in chromia was studied in both polycrystals and oxide films formed by oxidation of Ni–30Cr alloy in the temperature range of 700–1100 °C at an oxygen pressure equal to  $10^{-4}$  atm. Both bulk ( $D_b$ ) diffusion coefficients and grain-boundary diffusion ( $\alpha D_{\text{gb}}\delta$ ) parameters were determined for polycrystals and films. Moreover, in chromia films, due to the small grain size, effective diffusion coefficients were also deduced from the first part of the penetration curves.

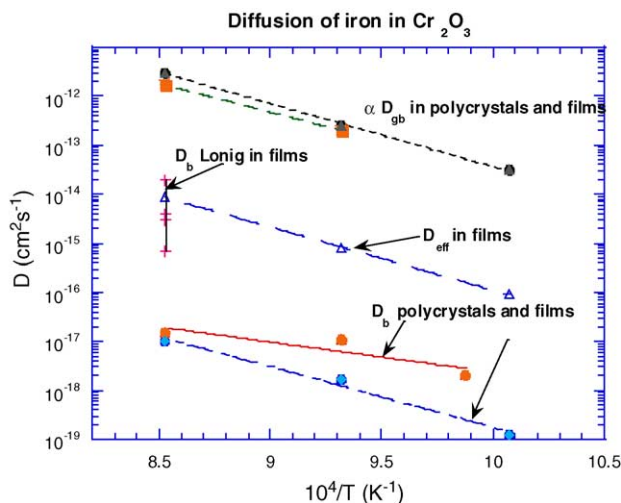


Fig. 10. Comparison, in an Arrhenius plot, of the diffusion coefficients given by Lobnig as bulk diffusion coefficients of iron in Cr<sub>2</sub>O<sub>3</sub> films and the iron diffusion coefficients in Cr<sub>2</sub>O<sub>3</sub> films determined in this work.

Iron diffusion does not really differ according to the microstructure of chromia. Bulk and grain-boundary diffusion coefficients are both of the same order of magnitude in chromia films and in chromia polycrystals. At the lowest temperatures, iron diffuses slightly faster in the bulk of polycrystals and inversely for diffusion along grain boundaries. Activation energy of grain-boundary diffusion is at least equal or greater than the values determined for bulk diffusion. Such abnormal results were already observed for other oxides and are probably associated to segregation phenomena along grain boundaries.

There is not a fundamental difference between iron diffusion and cationic self-diffusion in chromia films. However, along grain boundaries iron diffuses slightly slower than chromium and the difference increases when the temperature decreases.

These results indicate that the barrier effect played by chromia against other elements when used as a protective coating for high temperature materials is not only due to a diffusion effect. Even if it acts as a diffusion barrier when compared to nickel or iron oxides, it also decreases the oxygen potential at the inner interface of the chromia film and prevents other metallic elements from oxidizing. Thus, chromia films on metallic substrates also play a thermodynamic role which has an influence on the corrosion behaviour of alloys.

### Acknowledgements

The authors are grateful to CNPq and FAPEMIG (Brazil), and CNRS (France) for financial support.

### References

- [1] P. Kofstad, *High Temperature Corrosion*, Elsevier Applied Science, 1988.
- [2] V. Mousseaux, Doctor Thesis, University Paris VI, France, 1994.
- [3] A.C.S. Sabioni, B. Lesage, A.M. Huntz, J.C. Pivin, C. Monty, *Phil. Mag. A* 66 (1992) 333.
- [4] A.C.S. Sabioni, A.M. Huntz, F. Millot, C. Monty, *Phil. Mag. A* 66 (1992) 351.
- [5] A.C.S. Sabioni, A.M. Huntz, F. Millot, C. Monty, *Phil. Mag. A* 66 (1992) 361.
- [6] M.J. Graham, J.I. Elridge, D.F. Mitchell, R.J. Hussey, *Mater. Sci. Forum* 43 (1989) 207.
- [7] R.E. Lobnig, H.P. Schmidt, K. Hennessen, H.J. Grabke, *Oxidat. Met.* 37 (1992) 81.
- [8] S.C. Tsai, A.M. Huntz, C. Dolin, *Oxidat. Met.* 43 (1995) 581.
- [9] P. Moulin, A.M. Huntz, P. Lacombe, *Acta Metall.* 28 (1980) 745.
- [10] P. Faure, Thesis, INP Toulouse, France, 1979.
- [11] J. Philibert, *Atom Movements, Diffusion, and Mass Transport in Solids*, Les Editions de Physique, Les Ulis, France, 1991.
- [12] A.D. Le Claire, *Br. J. Appl. Phys.* 14 (1963) 351.
- [13] E.W. Hart, *Acta Metall.* 5 (1957) 597.
- [14] A. Atkinson, R.I. Taylor, *Phil. Mag. A* 43 (1981) 979.
- [15] S.C. Tsai, A.M. Huntz, C. Dolin, *Mater. Sci. Eng. A* 212 (1996) 6.
- [16] S.C. Tsai, Doctor Thesis, University Paris-XI, Orsay, France, 1996.
- [17] M. Le Gall, A.M. Huntz, B. Lesage, C. Monty, *Phil. Mag. A* 73 (1996) 919.
- [18] D. Prot, M. Le Gall, B. Lesage, A.M. Huntz, C. Monty, *Phil. Mag. A* 73 (1996) 935.
- [19] R.D. Shannon, *Acta Crystallogr. A* 32 (1976) 751.
- [20] K. Hoshino, N.L. Peterson, *J. Phys. Chem. Solids* 46 (1985) 1247.
- [21] A.M. Huntz, V. Bague, G. Beauplé, C. Haut, C. Sévérac, P. Lecour, X. Longaygue, F. Ropital, *Appl. Surf. Sci.* 207 (2003) 255.
- [22] A.M. Huntz, *J. Phys. III (France)* 5 (1995) 1729.